Physical Layer Specification of the L-band Digital Aeronautical Communications System (L-DACS1)

S. Brandes, U. Epple, S. Gligorevic, M. Schnell, German Aerospace Center (DLR), Germany
B. Haindl, M. Sajatovic, Frequentis AG, Austria

Abstract

L-DACS1 is the broadband candidate technology for the future L-band Digital Aeronautical Communications System (L-DACS). The flexible design of L-DACS1 allows the deployment as an inlay system in the spectral gaps between two adjacent channels used by the Distance Measuring Equipment (DME) as well as the non-inlay deployment in unused parts of the L-band. In this paper, the specification of the L-DACS1 physical layer enabling both the deployment as an inlay and as a non-inlay system is presented. Apart from the transmitter design, the design of the L-DACS1 receiver is addressed including methods for mitigating interference from other L-band systems. Special emphasis is put on channel estimation which has to be robust towards interference. The different proposed algorithms for channel estimation are evaluated in simulations of the overall L-DACS1 physical layer performance. The results show that L-DACS1 is capable of operating even under severe interference conditions, hence confirming the feasibility of the inlay concept.

Introduction

Within the future communication study (FCS) jointly carried out by Eurocontrol and the FAA, two candidates for the future L-DACS have been identified. The first candidate termed L-DACS1 is a broadband system employing Orthogonal Frequency-Division Multiplexing (OFDM) as modulation scheme and using Frequency-Division Duplex (FDD) for separating forward link (FL) and reverse link (RL). L-DACS1 has been anticipated to be a combination of P34 (TIA 902 standard) [1] and the Broadband Aeronautical Multi-carrier Communications (B-AMC) system [2-4]. L-DACS2 is a narrowband single-carrier system utilizing Time-Division Duplex (TDD) as duplex scheme. This system is a derivative of the L-band Digital Link (LDL) and the All-purpose Multi-channel Aviation Communication System (AMACS).

The FCS has recommended follow-on activities in order to further specify the proposed L-DACS options and validate their performance with the goal to finally decide for one candidate by 2010 [5]. These activities should be conducted within future research programs, i.e. Single European Sky ATM Research (SESAR) in Europe and NextGen in the USA. In 2008, Eurocontrol has initiated the specification for L-DACS1 which is the topic of this paper.

In [6], the air-ground (A/G) mode of L-DACS1 has been specified in detail, comprising a description of characteristics and capabilities of entire system, the specification of the ground and airborne L-DACS1 installations, the description of the L-DACS1 protocol architecture, as well as the specification of the L-DACS1 physical and medium access layers.

In this paper, special emphasis is put on the design of the physical layer. Since the L-band is already utilized by other systems like DME and free spectral resources are scarce and difficult to allocate, the preferred option for the L-DACS1 deployment is to operate it as an inlay system in the spectral gap between two adjacent channels assigned to the DME system. The small frequency separation of the two systems makes the design of the physical layer especially challenging. Furthermore, the design of the physical layer has to allow for alternatively deploying L-DACS1 without inlay in unused parts of the L-band.

The remainder of this paper is organized as follows. After a brief overview of L-DASC1 system capabilities and deployment options, the specification of the physical layer is presented. In addition to the design of the transmitter contained in the physical layer specification, the design of the receiver (Rx) is outlined in the next section. Special emphasis is put on channel estimation which has to be robust towards L-band interference when L-

DACS1 is deployed as an inlay system. Simulation results confirm the satisfactory overall system performance for the inlay deployment option under realistic interference and channel conditions. In the last section, conclusions are drawn.

System Overview

L-DACS1 offers two modes of operation, one for A/G communications and another one for air-air (A/A) communications. These two modes use different radio channels with different physical layer and data link layer approaches. So far, only the L-DASC1 A/G mode has been specified in detail [6] and will be recapitulated in the following.

System Capabilities

The L-DACS1 A/G sub-system is a multi-application cellular broadband system capable of simultaneously providing various kinds of Air Traffic Services (ATS) and Aeronautical Operational Control (AOC) communications services. It is designed to fulfill the requirements of the future aeronautical communication system as defined in [7].

The L-DACS1 A/G sub-system physical and data link layer are optimized for data communications, but the system also supports party-line voice communications, which are realized by re-transmissions via the ground station (GS).

The L-DACS1 A/G sub-system is a cellular point-to-multipoint system. The designed operational range is 200 nm. In order to limit the interference produced by the L-DACS1 transmitter, the maximum transmitting power shall be +41 dBm. The A/G mode assumes a star-topology with the L-DACS1 GS as a centralized instance that controls the L-DACS1 A/G communications within a certain volume of space, i.e. the L-DACS1 cell. The L-DACS1 GS can simultaneously support several bi-directional links to ASs under its control. Prior to utilizing the system an AS has to register at the controlling GS in order to get assigned dedicated logical channels for user and control data. Resources for control channels are statically allocated, while the resources for user channels are dynamically assigned according to the current demand.

Deployment Concept

L-DACS1 shall operate in the lower part of the L-band, i.e. 960 – 1164 MHz. FL and RL shall be separated by FDD. To build up a cellular system, multiple FL and RL channels each having an effective bandwidth of 498.05 kHz have to be found.

As depicted in Figure 1, the L-band is already utilized by several systems. Major parts are used by the DME system or the military Tactical Air Navigation (TACAN) system, both operating on a 1 MHz channel grid in the assigned sub-ranges. Additionally, parts of this band are used in some countries by the military Multifunctional Information Distribution System (MIDS) or the Joint Tactical Information Distribution System (JTIDS). Several fixed channels are allocated for the Universal Access Transceiver (UAT) at 978 MHz and for Secondary Surveillance Radar (SSR)/Airborne Collision Avoidance System (ACAS) at 1030 and 1090 MHz. In addition, fixed allocations have been made in the upper part of the L-band for the Global Positioning System (GPS) and Galileo. Commercial mobile communication systems such as the Universal Mobile Telecommunications System (UMTS) and the Global System for Mobile Communications (GSM) are operating immediately below the lower boundary of the aeronautical L-band (960 MHz).

When selecting channels for L-DACS1, co-location constraints have to be considered for the L-DACS1 AS. Additionally, the fixed L-band channels at 978, 1030, and 1090 MHz must be sufficiently isolated from L-DACS1 channels by appropriate guard bands.

One deployment option for L-DACS1 is the operation as an inlay system, i.e. L-DACS1 uses the spectral gaps between existing DME channels and operates at only 500 kHz offset to assigned DME channels. To relax co-site interference problems for an airborne L-DACS1 Rx, the frequency range 1048.5-1171.5 MHz, which is currently used by airborne DME interrogators, should be used for the RL. The proposed sub-range for the FL is 985.5 – 1008.5 MHz, i.e. at 63 MHz offset to the RL which corresponds to the DME duplex spacing.

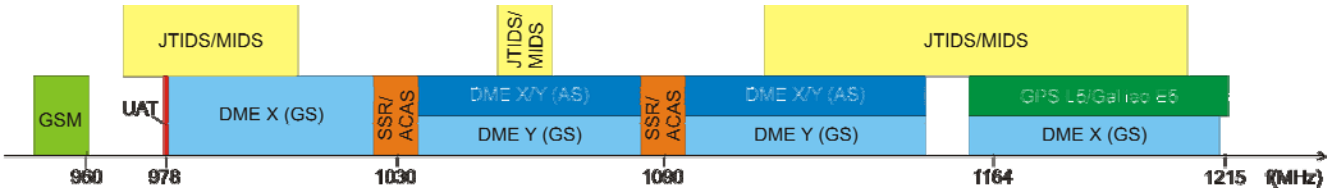

Figure 1: Current L-Band Usage

The inlay concept offers the clear advantage that it does not require new channel assignments and existing assignments can be retained unchanged. However, it poses a great challenge for the design of the L-DACS1 physical layer due to the small separation in frequency between L-DASC1 and DME resulting in strong interference between the two systems. On the one hand, the transmitted signal has to be designed such as to produce minimal out-of-band radiation that might disturb the DME and other L-band systems. On the other hand, the transmitted signal has to be robust towards interference and the Rx must be capable of mitigating the impact of severe interference from DME and other L-band systems [8].

Another deployment option is operating L-DACS1 as a non-inlay system in a sub-band of the aeronautical L-band that has been cleared for exclusive usage by L-DACS1. Alternatively, both deployment concepts can be combined, e.g. by realizing the inlay concept for the FL only and operating the RL in a free sub-band.

L-DACS1 has been designed to cope with the interference conditions expected in the inlay environment. The requirements on the future aeronautical communication system [7] are fulfilled even under strong interference conditions. However, the L-DACS1 design also allows a non-inlay or a mixed inlay/non-inlay deployment without any modifications. In that case, even higher system capacity and better performance are expected due to the substantially relaxed interference conditions.

PHY Layer Specification

The L-DACS1 physical layer is based on OFDM modulation and designed for operation in the aeronautical L-band (960 –1164 MHz). In order to maximize the capacity per channel and optimally use available spectrum, L-DACS1 is defined as a FDD system supporting simultaneous transmission in FL and RL channels, each with an effective bandwidth of 498.05 kHz.

L-DACS1 FL is a continuous OFDM transmission. Broadcast and addressed user data are transmitted on a (logical) data channel, dedicated control and signaling information is transmitted on (logical) control channels. The capacity/size of the data and the control channel changes according to system loading and service requirements. Message based adaptive transmission data profiling with adjustable modulation and coding parameters is supported for the data channels in FL and RL.

L-DACS1 RL transmission is based on OFDMA-TDMA bursts assigned to different users on demand. In particular, the RL data and the control segments are divided into tiles, hence allowing the medium-access control (MAC) sub-layer of the data link layer the optimization of resource assignments as well as the control of bandwidth and duty cycle according to the interference conditions.

OFDM parameters

The channel bandwidth of 498.05 kHz is used by an OFDM system with 50 sub-carriers, resulting in a sub-carrier spacing of 9.765625 kHz that is sufficient to compensate a Doppler spread of up to about 1.25 kHz typically occurring at aeronautical speeds. For OFDM modulation, a 64-point FFT is used. The total FFT bandwidth comprising all sub-carriers is 625.0 kHz.

According to the sub-carrier spacing, one OFDM symbol has a duration of 102.4 µs. Each OFDM symbol is extended by a cyclic prefix of 17.6 µs, comprising a guard interval of 4.8 µs for compensating multi-path effects as well as 12.8 µs for Tx windowing for reducing out-of-band radiation. This results in a total OFDM symbol

duration of 120 µs. The main L-DACS1 OFDM parameters are listed in Table 1.

Table 1: Main L-DACS1 OFDM Parameters

Parameter	Value
Effective bandwidth (FL or RL)	498.05 kHz
Sub-carrier spacing	9.765625 kHz
Used sub-carriers	50
FFT length	64
OFDM symbol duration	102.4 µs
Cyclic prefix - guard time - windowing time	17.6 µs 4.8 µs 12.8 µs
Total OFDM symbol duration	120 µs

OFDM Frames

The 64 sub-carriers contained in the FFT bandwidth can carry different types of symbols providing different functionalities:

- In most frame types, seven sub-carriers on the left and six on the right hand side of the spectrum carry null symbols and serve as guard bands. In addition, the sub-carrier in the center of the spectrum is not transmitted.
- Pilot symbols for channel estimation,
- Symbols that reduce the Peak-to-Average Power Ratio (PAPR),
- Synchronisation symbols used for time and frequency synchronization,
- Preamble symbols for facilitating automatic gain control (AGC),
- Data symbols used for data transmission.

Multiple OFDM symbols are organized into frames. Depending on their functionality, different frame types are distinguished. Moreover, different frame types are used in FL and RL.

FL OFDM Frame Types

In the FL, broadcast (BC) and combined Data/Common Control (CC) frames are utilized.

The FL Data/CC frame comprises 50 sub-carriers with 54 OFDM symbols, starting with 2 synchronization OFDM symbols followed by 52 OFDM symbols carrying data and pilot symbols. The total number of 158 pilot symbols results in a total data capacity of 2442 symbols per FL Data/CC frame. The mapping of CC information and data onto this frame type is described in the second next section.

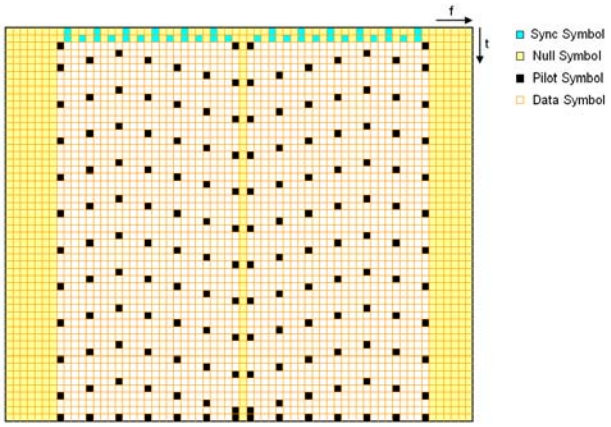

Figure 2: Structure of an FL Data/CC Frame

A FL BC frame consists of three consecutive sub-frames (BC1/BC2/BC3), in which the GS broadcasts signaling information to all active ASs within its coverage range. Figure 3 shows the structure of these sub-frames. The BC1 and BC3 sub-frames use 50 sub-carriers and contain two synchronization and 13 OFDM symbols each. Subtracting 48 pilot symbols, 602 symbols remain for data transmission. The BC2 sub-frame is 11 OFDM symbols longer than the BC1/3 sub-frame and provides a capacity of 1120 symbols.

Note, in the FL frames, no PAPR reduction symbols are inserted as the power amplifier used in the GS is assumed to provide sufficient linearity.

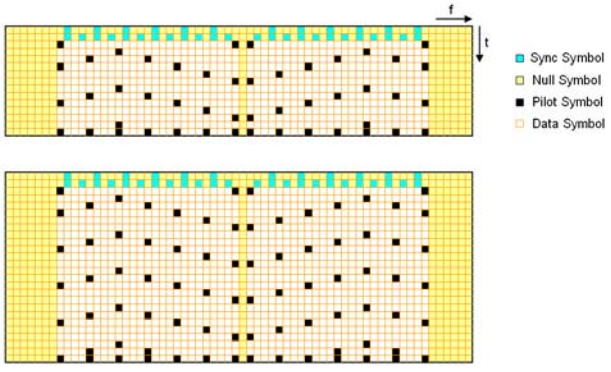

Figure 3: Structure of BC1 and BC3 Sub-Frames (above) and BC2 Sub-Frame (below)

RL OFDM Frame Types

To realize multiple-access via OFDMA-TDMA in the RL, the transmission is organized in segments and tiles rather than in OFDM frames and sub-frames as in the FL. The usage of tiles enables the optimization of the resource assignments by the MAC sub-layer. Furthermore, bandwidth and duty cycle can be optimally selected according to the interference conditions.

In the RL, data segments consist of tiles. As illustrated in Figure 4, one tile, representing the smallest allocation block in the RL, spans 25 symbols in frequency and 6 symbols in time direction in the time-frequency plane. It comprises 4 PAPR reduction symbols and 12 pilot symbols. This leads to a data capacity of 134 symbols per tile.

The PAPR reduction symbols carry complex numbers that have been optimized based on the data content such that the entire OFDM symbol, i.e. 24 data symbols and one PAPR reduction symbol, produces minimal PAPR. In the first and last OFDM symbol in a tile, PAPR is minimized by selecting the values for the pilot symbols such as to give minimal PAPR.

In the data segment, the tiles as depicted in Figure 4 are subsequently positioned left of the DC sub-carrier and mirrored versions of the tiles are positioned right of the DC sub-carrier. The length of the data segment is kept variable by allocating a variable number of tiles to the data segment. This structure also supports a flexible assignment of resources to different ASs by assigning different tiles or different blocks of subsequent tiles to different ASs.

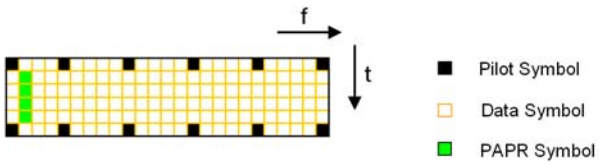

Figure 4: Structure of a Tile in the RL

Signaling information like resource allocation requests are transmitted in the dedicated control (DC) segment. A DC segment has the same tile structure as the RL data segment.

The first OFDM symbol of a DC segment carries an AGC preamble while the following K_{sy} OFDM symbols are reserved for synchronization sequences for the corresponding number of users. The minimal number of OFDM synchronization symbols is denoted by $K_{sy,min} = 5$. If more than five OFDM synchronization symbols per DC segment are required, K_{sy} can be increased in blocks of six. The OFDM synchronization symbols provide a possibility for the GS to update the synchronization of several ASs.

Within the remainder of the DC segment, exactly one tile is assigned to one AS. The length of a DC segment is variable. As an example, one DC segment comprising five OFDM synchronization symbols and six tiles is depicted in Figure 5.

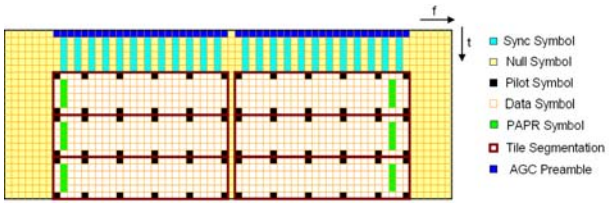

Figure 5: RL DC Segment

Two RL random access (RA) sub-frames provide two opportunities for ASs to send their cell entry request to the GS (Figure 6). Propagation guard times of up to $T_{g,RA} = 1.26$ ms precede and follow each RA sub-frame. The propagation guard time of 1.26 ms corresponds to a maximal AS-GS distance of 200 nm. When transmitting an RA sub-frame, an AS is not yet synchronized to the GS and the first RA sub-frame is transmitted directly after the start of an RL SF that in turn has been determined from the GS FL signal that needs 1.26 ms to reach an AS at the maximum distance from the GS. From the GS point of view, the first RL RA sub-frame is transmitted with 1.26 ms delay relative to the start of the first RA opportunity. Another propagation guard time of 1.26 ms is required for the RL RA sub-frame to reach the GS within the first RA opportunity. Similar considerations are valid for the second RA sub-frame that lags in time by 3.36 ms relative to the first one.

Figure 6: RA Access Opportunities

The RA sub-frame (Figure 7) contains seven OFDM symbols, resulting in a sub-frame duration of 840 µs.

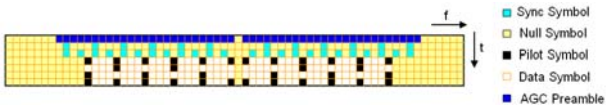

Figure 7: RL RA Sub-Frame

Framing Structure

In the FL, nine CC/Data frames are combined to one multi-frame (MF). The first four frames contain payload data. Data Physical layer Protocol Data Units (PHY-PDUs) are mapped onto these frames. Depending on the mode of Adaptive Coding and Modulation (ACM), the size of an FL Data PHY-PDU is 814 symbols, i.e. 1/3 of an FL Data/CC frame, or 162 symbols, i.e. 15 FL Data PHY-PDUs per frame and 12 remaining symbols.

The block with CC information starts with the beginning of the fifth frame and has a variable length that is steered by the number of FL CC PHY-PDUs. The size of an FL CC PHY-PDU is 814 symbols, i.e. 1/3 of an FL Data/CC frame, and 1-12 FL CC PHY-PDUs can be employed. The remainder of the MF is filled with FL Data PHY-PDUs with size corresponding to the applied ACM mode.

Each MF in the RL starts with an RL DC segment, followed by an RL data segment. The size of the DC segment, and thus also the size of the data segment is variable. The minimum size DC segment comprises an AGC symbol and five synchronization symbol opportunities followed by two tiles each containing a RL DC PHY-PDU. Since the extension of the DC segment over the entire MF is not reasonable, the maximum size of the DC segment is limited to 52 tiles. The remainder of the frame is filled up with the data segment.

The MF structure for FL and RL is shown in Figure 8. The reference synchronization point for the FL and RL is the beginning of the MF. It is noticeable, that FL CC PHY-PDUs and RL DC PHY-PDUs are transmitted interleaved rather than simultaneously. The temporal shift of the FL CC PHY-PDUs allows the requests sent in the RL DC PHY-PDUs to be answered already in the FL CC PHY-PDU of the same MF. Similarly, resource allocations transmitted in the FL CC PHY-PDU can already be used in the next RL MF.

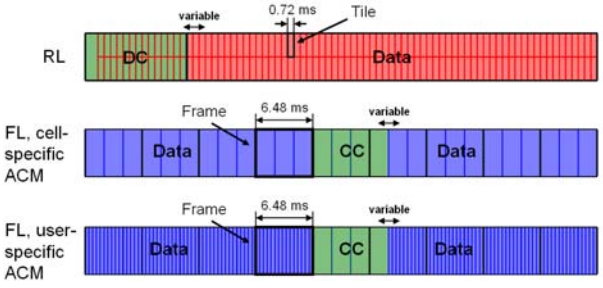

Figure 8: Multi-Frame Structure

On top of the MF structure, a super-frame (SF) structure is provided. In the FL, an SF contains a BC frame of duration 6.72 ms (56 OFDM symbols), and four MFs, each of duration 58.32 ms (486 OFDM symbols).

In the RL, each SF starts with a time slot of length T_{RA} = 6.72 ms with two opportunities for transmitting RL RA sub-frames followed by four MFs. The start of the FL BC frame is synchronized to the start of the RL RA.

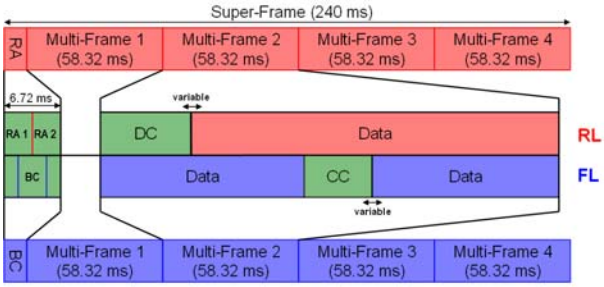

Figure 9: Super-Frame Structure

Coding and Modulation

To make the Tx signal robust towards interference a concatenated coding scheme consisting of a convolutional and a Reed-Solomon (RS) code is employed. The code rates and modulation schemes are adaptable to the current interference and channel conditions by ACM.

In the BC and CC PHY-PDUs in the FL and in the RA and DC PHY-PDUs in the RL always the basic coding and modulation scheme is used, i.e. quaternary phase-shift keying modulation (QPSK) and a rate 1/2 convolutional code in concatenation with a rate 0.9 RS code is applied.

For the transmission of data, ACM is provided in both FL and RL. In the FL, two ACM modes are defined:

- Cell-specific ACM mode, which means that data for all users within the cell are encoded and modulated with a fixed scheme, and
- User-specific ACM mode, which means that separate coding and modulation schemes are applied to data of different users.

In case of cell-specific ACM, the information about the chosen coding and modulation scheme is transmitted in the BC frame. In case of user-specific ACM the GS transmits the information about coding and modulation for the different ASs via the coding and modulation scheme FL map in the CC information block.

In the RL, user-specific ACM is supported only for data segments. The selection of a coding and modulation scheme for a certain AS is carried out by the GS and communicated when assigning resources to this AS.

The coding and modulation rate is varied by employing different modulation schemes and different code rates for the convolutional code. Three modulation schemes, namely QPSK, 16-quadrature amplitude modulation (QAM), and 64-QAM are available. The rate of the convolutional code can be changed from 1/2 to 2/3 or 3/4, resulting in a total of 8 different coding and modulation schemes.

Taking into account overhead within the OFDM frames due to synchronization and pilot symbols as well as typical overhead in the frame structure due to the transmission of control information, the data rates provided on FL and RL can be calculated. With two CC PHY-PDUs resulting in 25 Data PHY-PDUs per MF, data rates ranging from 303.3 kbit/s to 1373.3 kbit/s can be achieved on the FL. Assuming the DC segment to contain 20 tiles, the aggregate data rate for all users on the RL varies from 220.3 to 1038.4 kbit/s.

Reduction of Out-of-Band Radiation

High out-of-band OFDM sidelobes may cause harmful interference at the Rx of other L-band systems and have to be reduced. For that purpose, Tx windowing is applied in order to smooth the sharp phase transitions between consecutive OFDM symbols which cause out-of-band radiation.

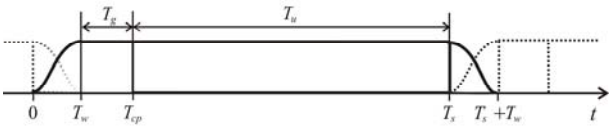

Figure 10: Tx Windowing Function

As illustrated in Figure 10, the OFDM symbol with duration T_u is extended by a cyclic prefix of length T_{cp}. One part of the cyclic prefix of length T_g serves as guard interval to compensate multi-path propagation on the radio channel. The second part of length T_w contains the leading edge of the window. In addition, the OFDM symbol is extended by a cyclic suffix of length T_w which contains the trailing edge of the window. With this approach it is guaranteed that Tx windowing does not affect the useful part of the OFDM symbol including guard interval. To keep the overhead induced by extending the OFDM symbol duration at a minimum, subsequent OFDM symbols overlap in those parts containing the leading and trailing edges of the window. For L-DACS1, a raised-cosine window with roll-off factor $\alpha = 0.107$ is proposed hence requiring a window time T_w of 12.8 μs.

Receiver Design

Interference Mitigation

When deployed as an inlay system, signals of existing L-band systems may cause severe interference onto the L-DACS1 Rx. Especially DME systems operating at small frequency offset to the L-DACS1 channel represent a source of strong interference. Two promising techniques, aiming at mitigating the influence of interference onto L-DACS1, are presented in the following.

Over-Sampling

RF and IF filters in the selective stages of the L-DACS1 Rx successively reduce interference contributions received outside the L-DACS1 bandwidth. Since the interference signal power can be very high, it may not be possible to completely remove this out-of-band interference power. In particular, due to the relatively large occupied bandwidth of the DME signal, the spectra of DME

Txs operating at ±0.5 MHz offset from the L-DACS1 channel partly fall into the L-DASC1 Rx bandwidth.

Subsequent sampling of the filtered Rx signal in the A/D-converter with sampling period $T_{sa} = 1/B_{FFT}$ leads to periodic repetitions of the interference spectra in the frequency domain in distances $k * B_{FFT}$, $k \in \mathbb{Z}$. In the case without interference, the filtered Rx signal is band-limited by B_{FFT}. Sampling with $T_{sa} = 1/B_{FFT}$ does not lead to aliasing effects. However, the Nyquist sampling theorem is not fulfilled for the interference signal. The remaining out-of-band interference signal is not band-limited to B_{eff} and when applying the FFT at the OFDM Rx due to aliasing undesired signal parts would fall into the L-DACS1 bandwidth. This can be avoided by over-sampling the time domain Rx signal at least by a factor of 4, resulting in an increased spacing between the periodic repetitions in the frequency domain and reduced aliasing effects. The over-sampled Rx signal is then transformed to the frequency domain by an FFT with size increased according to the over-sampling factor. For further signal processing, only the relevant sub-carriers in the L-DACS1 system bandwidth are considered. All other sub-carriers are discarded.

Pulse Blanking

Pulse blanking (PB) is a well-known approach for reducing pulsed interference such as DME interference. It has already been applied for reducing DME interference in the E5- and L5-bands used by satellite navigation systems [9] and for reducing impulsive noise in OFDM systems [10].

In L-DACS1, PB is applied to the digitised Rx signal after A/D conversion. When the amplitude of the over-sampled Rx signal exceeds the threshold T_{PB} the corresponding samples are blanked, i.e. set to zero.

Besides the DME interference, the blanked samples also comprise the desired OFDM signal and noise. Hence, the threshold T_{PB} has to be chosen carefully. When choosing it too low, the corruption of the desired signal exceeds the benefit of reducing the interference power, whereas a too high threshold leads to a strong remaining interference power. A suitable criterion for optimally setting T_{PB} is the signal-to-noise-and-interference ratio (SINR) [10].

Due to high PAPR in OFDM systems, peaks of the desired OFDM signal and DME pulses cannot be clearly distinguished. For an unambiguous detection of interference pulses in the Rx signal, a correlation of the Rx signal with a known interference pulse has been proposed in [11]. Compared to PB based on the perfectly known interference signal, in most cases the same number of samples is blanked in the Rx signal. Thus, in the following, perfect pulse detection based on the actual interference signal is assumed.

Channel Estimation

As basic channel estimation algorithm in L-DACS1, a pilot-aided linear interpolation is proposed. In order to make channel estimation robust towards interference, the pilot pattern depicted in Figure 2 has been specified for L-DACS1 FL Data/CC frames. As this paper focuses on the channel estimation when transmitting user data, the pilot pattern of the BC and RA frames are not considered. In time direction, the distance between pilot tones is set to five, except for the beginning and the end of a frame. In frequency direction, pilot tones are spread over all sub-carriers in order to reduce the number of pilot tones that would be affected by strong DME interference from the adjacent DME channel. The distance of sub-carriers which contain pilot tones can be given by four. These pilot distances have been chosen in accordance with the expected Doppler shifts and maximal delay times in the case of multi-path propagation. This results in the pilot pattern depicted in Figure 4. The distance between pilot tones in time direction is set to five like in the FL. In frequency direction, the distance between pilot tones is five at the edges of the spectrum. Otherwise it is set to four.

In the RL, where different tiles can be assigned to different users, channel estimation must be performed tile-based.

The algorithm recommended for L-DACS1 channel estimation consists of an interpolation in time direction and a subsequent interpolation in frequency direction. Based on the channel coefficients at pilot positions, e.g. $\tilde{H}_p[\upsilon]$ and $\tilde{H}_{p+\lambda}[\upsilon]$, with λ being the distance of two adjacent pilot tones in time direction, the channel

coefficients at data positions in between are calculated by

$$\tilde{H}_{p+i}[\upsilon] = \frac{\lambda - i}{\lambda}\hat{H}_p[\upsilon] + \frac{i}{\lambda}\hat{H}_{p+\lambda}[\upsilon], \quad i = 1,...,\lambda - 1 \tag{1}$$

This one-dimensional interpolation is applied to all sub-carriers containing pilot tones.

In FL Data/CC frames, an additional interpolation of the channel coefficients in the second synchronisation symbol has to be applied. These channel coefficients have to be used for estimating the channel coefficients in time direction on the sub-carriers with index υ = [-21, -17, -13, -9, -5, 5, 9, 13, 17, 21] relative to the DC sub-carrier, since the first data OFDM symbol does not contain pilot tones on these sub-carriers.

Based on the channel coefficients at pilot positions and the channel coefficients calculated in the first step, the missing channel coefficients on non-pilot sub-carriers are calculated in the second step by a one-dimensional interpolation in frequency direction. Eq. (1) also holds for this procedure by simply changing p and υ. In this interpolation step, $\tilde{H}_p[\upsilon]$ from Eq. (1) comprises not only channel coefficients at pilot positions, but also channel coefficients at data positions which have been estimated in the first step.

Wiener-interpolation has been investigated as another algorithm for channel estimation. Like for the linear interpolation, the estimation is split up into an interpolation in time and another in frequency direction. Since Wiener-interpolation is a non-linear procedure, the result will not be as good as two-dimensional estimation in time- and frequency direction. However, as shown in [12], the differences are minimal. The detailed description of the algorithm for one-dimensional Wiener-interpolation for OFDM can be found in [13].

To improve channel estimation, pilot boosting in the FL can be applied. In this case, the power of the pilot symbols is increased to 2.5 dB over the average power of data symbols. To guarantee a constant average power of the transmission, the power of the data symbols is reduced accordingly, leading to a decreased SNR on the data bearing sub-carriers.

In the RL, no pilot boosting is applied as the pilot tones are concentrated in the first and last OFDM symbol of each tile. As a constant transmit power of each OFDM symbol is desired, a large number of power boosted pilot symbols within one OFDM symbol has to be compensated with a remarkable lower power of the data symbols in the same OFDM symbol. These data symbols would dominate the bit error rate (BER).

A further improvement of the channel estimation in the case of DME interference is pilot erasure setting, which is based on the idea of erasure decoding [8]. When strong DME interference coincidences with a pilot tone in the frequency domain, this pilot symbols will produce a wrong contribution to the calculation of the channel coefficients. By pilot erasure setting these channel coefficients are set to zero. The idea behind is that for a particular pilot symbol, no information about the channel is better than unreliable information. For setting the pilot erasures, a reliable detection and estimation of DME interference in the frequency domain is essential. The detection is provided on some of the unused guard sub-carriers at each side of the spectrum. On these sub-carriers, the interference power level is measured and the interference signal on the pilot tones is reconstructed based on known spectral characteristics of DME signals [8].

In the FL, these erased channel coefficients may also be reconstructed using adjacent pilot tones on the same sub-carrier:

$$\hat{H}_{p_0}[\upsilon_0] = \frac{1}{2}\hat{H}_{p_0-\lambda}[\upsilon_0] + \frac{1}{2}\hat{H}_{p_0+\lambda}[\upsilon_0], \tag{2}$$

with p_0 being an OFDM symbol which is hit by DME interference, distorting the pilot tone on sub-carrier υ_0. λ corresponds to the distance of pilot tones in time direction.

Simulation Results

Assuming the inlay deployment concept, the impact of DME interference in the FL is simulated for an interference scenario representing severe interference conditions. The L-DACS1 FL is intended to be operated in the sub-band 979-1025 MHz. Except for co-site interference from the "own" airborne DME interrogator, which is

neglected here, only DME GSs cause interference at the L-DACS1 airborne Rx. The real DME channel allocation is modeled with the NAVSIM[1] tool [14] for the area with the highest density of DME ground stations in Europe. The victim L-DACS1 Rx is positioned at an en-route flight level at 45,000 feet altitude in the center of this area. The peak interference power originating from each DME/TACAN GS is determined via simple link budget calculations, taking into account free space loss and elevation angle dependent antenna gains that are derived from directive antennas of standard DME equipment. In this particular example, severe interference conditions are observed when L-DACS1 is operated at 995.5 MHz. In the scenario given in Table 2, only interferers in the channels at ±0.5 MHz offset to the L-DACS1 center frequency are considered. Interference from DME stations in channels at larger offsets are supposed not to impair L-DACS1 significantly due to their larger separation in frequency.

Table 2: Interference Scenario

Station	Frequency (MHz)	Interference power at victim Rx input	Pulse rate (ppps)
TACAN	995	-67.9 dBm	3600
L-DACS1	995.5		
TACAN	996	-74.0 dBm	3600
TACAN	996	-90.3 dBm	3600

The performance of the channel estimation is investigated in an aeronautical environment, assuming a maximal Doppler shift of 1250 Hz which corresponds to a velocity of 1360 km/h. Besides a strong line-of-sight path, reflected paths with a delay of $\tau_1 = 0.3\mu s$ and $\tau_2 = 15\mu s$ occur.

In Figure 11, the mean square error (MSE) of the channel coefficients estimated by linear interpolation with and without pilot boosting is given versus SNR in the case of no interference and the interference scenario from Table 2. Compared to the interference-free case, in the case of interference, the MSE of the linear interpolation degrades by 55% for nearly all SNR values. Pilot boosting leads to 35% improvement of the MSE of the channel estimation in both cases with and without interference.

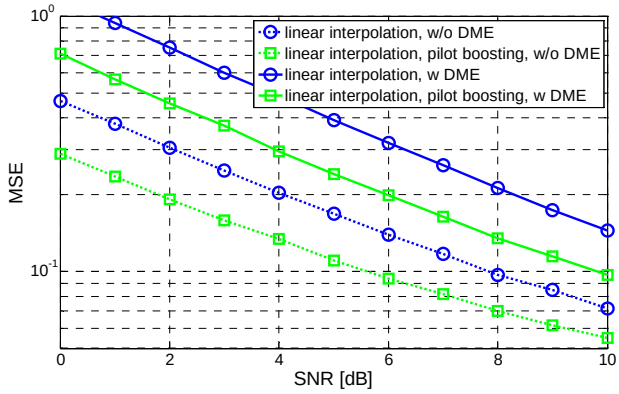

Figure 11: MSE of Channel Estimation in the FL

The corresponding BER curves are given in Figure 12. The gain of pilot boosting is not as high as expected from the MSE curves, since pilot boosting leads to a lower signal energy of the data symbols, which is not taken into account when considering MSE curves. However, the gain of pilot boosting in the case of interference is still 0.8 dB at BER = 10^{-3}.

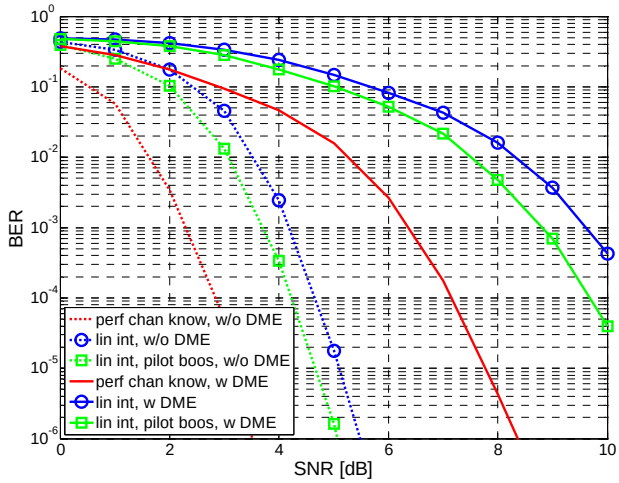

Figure 12: BER Performance of Channel Estimation in the FL

In addition, curves assuming perfect knowledge of the channel are given as reference. For an interference-free transmission, the perfect channel knowledge can be approached by 1.4 dB at BER = 10^{-3} with linear interpolation and pilot boosting. However, with DME interference, the gap between these two cases increases to 2.4 dB at BER = 10^{-3}.

[1] The Air Traffic / ATC & CNS simulation tool "NAVSIM" has been developed by "Mobile Communications R&D GmbH, Salzburg" in close co-operation with University of Salzburg.

For decreasing this fairly wide performance gap between perfect channel knowledge and linear interpolation, the methods described in the channel estimation section are investigated. Figure 13 shows the MSE curves when additionally applying PB, pilot erasure setting, or pilot reconstruction, respectively.

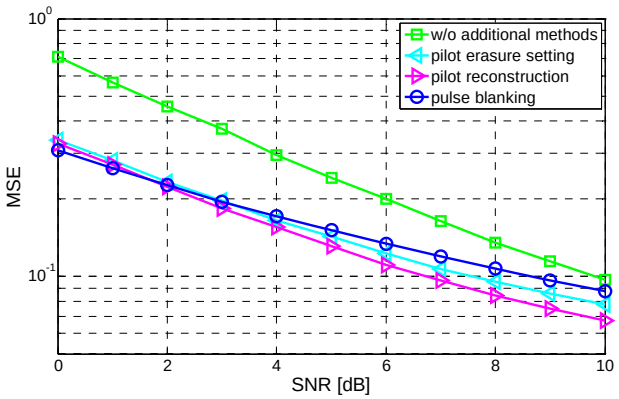

Figure 13: MSE of Linear Interpolation and Pilot Boosting in the FL with Interference

All three methods lead to a noticeable reduction of the MSE. However, there are some differences. The gain with PB reduces from 50% at SNR = 2 dB to 20% at SNR = 8 dB. Besides the desired reduction of interference, PB leads to undesired inter-carrier-interference (ICI). For low SNR values, i.e. strong DME interference, the beneficial influence of removing the interference power prevails, whereas for high SNR values ICI becomes noticeable, hence leading to lower gains. When applying pilot erasures, the reduction of the MSE is still 30% and for pilot reconstruction 37% at SNR = 8 dB, as these methods do not cause ICI.

The corresponding BER curves are given in Figure 14. While pilot reconstruction, compared to pilot erasure setting, leads to a better MSE of the channel estimation, the BER is worse. When an OFDM symbol is hit by strong DME interference from the adjacent channel, pilot tones as well as data symbols at the edge of the L-DACS1 spectrum are destroyed. Thus, even reconstructed pilot tones will not lead to correctly equalized data. When setting pilot tones to zero, the interpolated channel coefficients are lower, resulting in equalized data with lower reliability. When demodulating and decoding, a lower reliability of corrupted equalized data leads to a better performance. The gap between perfect channel knowledge and linear interpolation is reduced to 0.4 dB at BER = 10^{-3}.

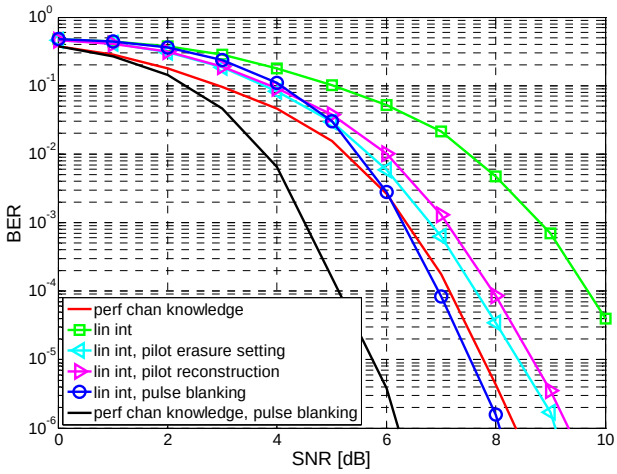

Figure 14: BER Performance of Channel Estimation with Pilot Boosting in the FL with Interference

A comparison of these methods with PB in terms of BER is difficult, as PB also influences data symbols. Thus, PB combined with linear interpolation is compared to PB assuming perfect channel knowledge. The degradation of the linear interpolation is 1.7 dB at BER = 10^{-3}. This fairly high loss results from ICI, which leads to corrupted channel coefficients in the linear interpolation.

Conclusions and Outlook

L-DACS1 is the broadband candidate for the future A/G communication system in the L-band. It is designed to meet the requirements of the future aeronautical communication system. The flexible design of L-DACS1 allows the deployment as an inlay system in the spectral gap between two adjacent DME channels as well as the deployment in unused spectrum.

In the first part of this paper, the recently published system specification is recapitulated, with focus put on the physical layer. The basic OFDM parameters as well as different frame types are described. The framing structure for FL and RL comprises a sequence of different types of frames and segments that allows for flexibly adapting the transmission of control and user data with different data rates to the current demands.

In the second part, the Rx design is addressed. To combat interference from other L-band systems in an inlay system, interference mitigation has to be applied at Rx. Since channel estimation is also affected by interference, the pattern of pilot symbols in the OFDM frames and tiles has been designed such as to make channel estimation robust towards interference. It is shown that a pilot-aided linear interpolation leads to good results in an interference-free environment. In the case of interference, additional methods such as pilot boosting and pilot erasure setting have been applied, leading to a system performance close to that achievable with perfect channel knowledge.

References

[1] TIA standard family TIA-902, 2002/2003

[2] M. Schnell, S. Brandes, S. Gligorevic, C.-H. Rokitansky, M. Ehammer, Th. Gräupl, C. Rihacek, M. Sajatovic, "B-AMC – Broadband Aeronautical Multi-carrier Communications", *2008 Integrated Comm. Navigation and Surveillance Conf. (ICNS 2008)*, Bethesda, MD, USA, May 2008

[3] C.-H. Rokitansky, M. Ehammer, Th. Gräupl, M. Schnell, S. Brandes, S. Gligorevic, C. Rihacek, and M. Sajatovic, "B-AMC - A system for future Broadband Aeronautical Multi-Carrier communications in the L-Band," *2007 Digital Avionics Systems Conference (DASC 2007)*, Dallas, TX, USA, October 2007, pp. 4.D.2-1- 4.D.2-13

[4] C.-H. Rokitansky, M. Ehammer, T. Gräupl, S. Brandes, S. Gligorevic, M. Schnell, C. Rihacek, and M. Sajatovic, "B-AMC – Aeronautical Broadband Communication in the L- band," in *Proc. CEAS European Air and Space Conference '07*, Berlin, Germany, Sept. 2007, pp. 487-496

[5] AP17 Final Conclusions and Recommendations Report, EUROCONTROL/FAA/ NASA, v1.1, November 2007

[6] M. Sajatovic, B. Haindl, M. Ehammer, Th. Gräupl, M. Schnell, U. Epple, S. Brandes, "L-DACS1 System Definition Proposal", Eurocontrol Study, Edition 1.0, February 2009

[7] EUROCONTROL/FAA, "Communications Operating Concept and Requirements for the Future Radio System", Ver. 2, May 2007

[8] M. Schnell, S. Brandes, S. Gligorevic, M. Walter, C. Rihacek, M. Sajatovic, B. Haindl, "Interference Mitigation for Broadband L-DACS", *2008 Digital Avionics Systems Conference (DASC 2008)*, St. Paul, MN, USA, October 2008

[9] G. X. Gao, "DME/TACAN Interference and its Mitigation in L5/E5 Bands," in *ION Institute of Navigation Global Navigation Satellite Systems Conference*, Fort Worth, TX, USA, September 2007

[10] S. V. Zhidkov, "Performance Analysis and Optimization of OFDM Receiver with Blanking Nonlinearity in Impulsive Noise Environment," *IEEE Transactions on Vehicular Technology*, vol. 55, no. 1, pp. 234–242, January 2006

[11] S. Brandes and M. Schnell, "Interference Mitigation for the Future Aeronautical L-Band Communication System," *7th International Workshop on Multi-Carrier Systems & Solutions (MC-SS 2009)*, Herrsching, Germany, May 2009

[12] P. Hoeher, S. Kaiser, and P. Robertson, "Two-Dimensional Pilot-Symbol-Aided Channel Estimation by Wiener Filtering," *IEEE Intl. Conference on Acoustics, Speech, and Signal Processing,* vol. 3, pp. 1845, April 1997

[13] P. Hoeher, "TCM on frequency-selective land-mobile fading channels," *Proc. 5th Tirrenia Intl. Workshop on Digital Comm.,* Tirrenia, Italy, pp. 317-328, Sept. 1991

[14] EUROCONTROL, "VDL Mode 2 Capacity Analysis through Simulations, WP3.B – NAVSIM Overview and Validation Results", Edition 1.2, Oct. 2005

Email Addresses

sinja.brandes@dlr.de

ulrich.epple@dlr.de

snjezana.gligorevic@dlr.de

michael.schnell@dlr.de

Bernhard.HAINDL@frequentis.com

Miodrag.SAJATOVIC@frequentis.com